Final charged-lepton angular distribution and possible anomalous top-quark couplings in $pp \to t\bar{t}X \to \ell^+X'$

arXiv:1406.2475v1 [hep-ph] 10 Jun 2014

Zenrō HIOKI [1), a)] and Kazumasa OHKUMA [2), b)]

1) *Institute of Theoretical Physics, University of Tokushima*
Tokushima 770-8502, Japan

2) *Department of Information and Computer Engineering,*
Okayama University of Science
Okayama 700-0005, Japan

ABSTRACT

Possible anomalous (or nonstandard) top-quark interactions with the gluon and those with the W boson induced by $SU(3) \times SU(2) \times U(1)$ gauge-invariant dimension-6 effective operators are studied in $pp \to t\bar{t}X \to \ell^+X'$ ($\ell = e$ or μ) at the Large Hadron Collider (LHC). The final charged-lepton (ℓ^+) angular distribution is first computed for nonvanishing nonstandard top-gluon and top-W couplings with a cut on its transverse momentum. The optimal-observable procedure is then applied to this distribution in order to estimate the expected statistical uncertainties in measurements of those couplings that contribute to this process in the leading order.

PACS: 12.38.Qk, 12.60.-i, 14.65.Ha

[a)] E-mail address: hioki@tokushima-u.ac.jp
[b)] E-mail address: ohkuma@ice.ous.ac.jp

1. Introduction

The Large Hadron Collider (LHC) at CERN has been presenting us fruitful experimental data on various particles/processes ever since it started operating, of course including the historic discovery of the/a Higgs boson [1]. Exploring possible new physics beyond the standard model (BSM) is also an important mission of the LHC. Although they have not found so far any exciting signals indicating BSM yet, this fact never means that there do not exist exotic particles since their masses might be too high to be directly produced there.

Even in such a case, we still would be able to investigate certain new-physics effects indirectly, using data from the LHC. For example, we have studied possible nonstandard chromomagnetic and chromoelectric dipole moments of the top-quark (denoted as d_V and d_A respectively) in Refs.[2]–[4], and obtained much stronger restrictions on them than before[♯1] by adding the data on the $t\bar{t}$ total cross sections from the LHC to those from the Tevatron. We then carried out an optimal-observable analysis (OOA) to show how precisely we could determine those nonstandard couplings in $pp \to t\bar{t}X \to \ell^+X'$ ($\ell = e$ or μ) under a linear approximation by using the ℓ^+ angular and energy distributions, where we also took into account possible nonstandard top-W coupling (denoted as d_R) [5]. There, however, we were not able to study the d_R contribution through the angular distribution due to the decoupling theorem [6]–[8].

The d_R dependence of this distribution recovers if we perform the energy integration necessary to derive it in some limited range, as will be discussed later. The purpose of this article is to study if we could thereby draw any new information on d_R via a similar OOA: After summarizing our calculational framework, we are going to clarify to what extent the distribution becomes dependent of this parameter by computing it for some different d_R values with a ℓ^+ transverse-momentum ($p_{\ell\,\mathrm{T}}$) cut. Then we apply the optimal-observable procedure to this distribution with and without the d_V-term contribution. Concerning the ℓ^+ energy distribution, on the other hand, we do not re-study it here because that distribution is d_R-dependent from the beginning and therefore adding the $p_{\ell\,\mathrm{T}}$ cut does not bring us anything

[♯1] As for the preceding analyses, see the reference lists of [2]–[4].

essentially-new in comparison with what we have done in [5].

2. Framework

The framework of our model-independent analyses is based on an effective-Lagrangian whose low-energy form reproduces the standard-model (SM) interactions. This is one of the most promising methods to describe new-physics phenomena when the energy of our experimental facility is not high enough to produce new particles. Assuming any non-SM particles too heavy to appear as real ones, we take the following effective Lagrangian:

$$\mathcal{L}_{\rm eff} = \mathcal{L}_{\rm SM} + \frac{1}{\Lambda^2}\sum_i \left(C_i\mathcal{O}_i + \text{h.c.} \right), \tag{1}$$

where $\mathcal{L}_{\rm SM}$ is the SM Lagrangian, $\mathcal{O}_i$ mean $SU(3)\times SU(2)\times U(1)$ gauge-invariant operators of mass-dimension 6 involving only the SM fields and their coefficients C_i parameterize virtual effects of new particles at an energy less than the assumed new-physics scale Λ. Note here that the dimension-6 operators give the largest contributions in relevant processes as long as we assume the lepton-number conservation. In this framework, all the form factors related to C_i are dealt with as constant parameters, without supposing any specific new-physics models.

All those dimension-6 operators have been arranged in Refs.[9]–[12]. Following the notation of [11], the effective Lagrangian for the parton-level process $q\bar{q}/gg \to t\bar{t} \to b\bar{b}W^+W^-$ is given in [3] as

$$\mathcal{L}_{\rm eff} = \mathcal{L}_{t\bar{t}g,gg} + \mathcal{L}_{tbW} \tag{2}$$

$$\mathcal{L}_{t\bar{t}g,gg} = -\frac{1}{2}g_s\sum_a\Big[\,\bar{\psi}_t(x)\lambda^a\gamma^\mu\psi_t(x)G^a_\mu(x) - \bar{\psi}_t(x)\lambda^a\frac{\sigma^{\mu\nu}}{m_t}\big(d_V + id_A\gamma_5\big)\psi_t(x)G^a_{\mu\nu}(x)\,\Big], \tag{3}$$

$$\mathcal{L}_{tbW} = -\frac{1}{\sqrt{2}}g\Big[\,\bar{\psi}_b(x)\gamma^\mu(f_1^LP_L + f_1^RP_R)\psi_t(x)W^-_\mu(x) + \bar{\psi}_b(x)\frac{\sigma^{\mu\nu}}{M_W}(f_2^LP_L + f_2^RP_R)\psi_t(x)\partial_\mu W^-_\nu(x)\,\Big], \tag{4}$$

where g_s and g are the $SU(3)$ and $SU(2)$ coupling constants, $P_{L/R} \equiv (1\mp\gamma_5)/2$, d_V, d_A and $f_{1,2}^{L,R}$ are form factors defined as

$$d_V \equiv \frac{\sqrt{2}vm_t}{g_s\Lambda^2}\text{Re}(C^{33}_{uG\phi}), \quad d_A \equiv \frac{\sqrt{2}vm_t}{g_s\Lambda^2}\text{Im}(C^{33}_{uG\phi}),$$

$$f_1^L \equiv V_{tb} + C_{\phi q}^{(3,33)*}\frac{v^2}{\Lambda^2}, \qquad f_1^R \equiv C_{\phi\phi}^{33*}\frac{v^2}{2\Lambda^2}, \tag{5}$$
$$f_2^L \equiv -\sqrt{2}C_{dW}^{33*}\frac{v^2}{\Lambda^2}, \qquad f_2^R \equiv -\sqrt{2}C_{uW}^{33}\frac{v^2}{\Lambda^2}$$

with v being the Higgs vacuum expectation value and V_{tb} being the (tb) element of Kobayashi–Maskawa matrix. Among those unknown parameters, d_V and d_A are respectively the top-quark chromomagnetic and chromoelectric dipole moments, and we use d_R defined as

$$d_R \equiv \mathrm{Re}(f_2^R)M_W/m_t \tag{6}$$

instead of f_2^R in order to make our formulas a little bit simpler.

In the following work, we use the above effective Lagrangian for top-quark interactions, and adopt the linear approximation for those nonstandard parameters as in [5], where d_V and d_R come into our analyses (note that d_A terms do not contribute to $q\bar{q}/gg \to t\bar{t}$ in the leading order because of their CP-odd property). We assume the other interactions, e.g. the one for $W^+ \to \ell^+\nu$, are described by the usual SM Lagrangian, and all the fermions lighter than the top quark are treated as massless particles. Concerning the parton distribution functions, we have been using CTEQ6.6M (NNLO approximation) [13].

3. Lepton angular distribution and decoupling theorem

What we call "the decoupling theorem" is a theorem which states that the leading contribution of the anomalous top-decay couplings, d_R in our case, to final-particle angular distributions vanishes when only a few conditions are satisfied [6]–[8]. In terms of the ℓ^+ angular distribution under consideration, this theorem holds if we assume the standard $V-A$ structure for the $\nu\ell W$ coupling and perform the lepton-energy integration fully over the kinematically-allowed range. As a result, this distribution becomes exclusively dependent of d_V. That is, we can no longer get any information thereby on the nonstandard top-decay coupling d_R.

Although it is not possible to cover the full phase space of the final-lepton momentum in actual experiments, we could carry out the above energy integration using the energy distribution reconstructed through a proper extrapolation. Therefore the above-mentioned full integration is not unrealistic. This however tells us

that we might be able to draw certain new information on d_R by using the angular distribution with some cut on the lepton momentum.

Let us calculate the ℓ^+ angular distribution with a ℓ^+ transverse-momentum ($p_{\ell\,\mathrm{T}}$) cut as a typical and realistic experimental condition. We first take one of the proton beams as the base axis and express the differential cross section of $pp \to t\bar{t}X \to \ell^+ X'$ (the angular and energy distribution of ℓ^+) in the proton-proton CM frame as follows:

$$\frac{d^2\sigma_\ell}{dE_\ell\, d\cos\theta_\ell} = f_{\mathrm{SM}}(E_\ell, \cos\theta_\ell) + d_V f_{d_V}(E_\ell, \cos\theta_\ell) + d_R f_{d_R}(E_\ell, \cos\theta_\ell), \tag{7}$$

where E_ℓ is the lepton energy, θ_ℓ is the lepton scattering angle, i.e., the angle formed by the ℓ^+ momentum and the above-mentioned base axis, $f_{\mathrm{SM}}(E_\ell, \cos\theta_\ell)$ denotes the SM contribution, and the other two $f_I(E_\ell, \cos\theta_\ell)$ describe the non-SM terms corresponding to their coefficients. The explicit forms of $f_I(E_\ell, \cos\theta_\ell)$ at the parton level are easily found in the relevant formulas in [3]. Then, the ℓ^+ angular distribution is written as

$$\frac{d\sigma_\ell}{d\cos\theta_\ell} = g_1(\cos\theta_\ell) + d_V\ g_2(\cos\theta_\ell) + d_R\ g_3(\cos\theta_\ell), \tag{8}$$

where $g_i(\cos\theta_\ell)$ are given by

$$g_i(\cos\theta_\ell) = \int dE_\ell\ f_I(E_\ell, \cos\theta_\ell) \tag{9}$$

with $i = 1, 2$ and 3 corresponding to $I = \mathrm{SM}$, d_V and d_R, respectively. In the above E_ℓ integration, the kinematically-allowed range is

$$\frac{M_W^2}{\sqrt{s}(1+\beta)} \le E_\ell \le \frac{m_t^2}{\sqrt{s}(1-\beta)} \tag{10}$$

with $\beta \equiv \sqrt{1 - 4m_t^2/s}$. As mentioned, $g_3(\cos\theta_\ell)$ disappears if we perform the integration fully over this range due to the decoupling theorem.

We compute this angular distribution for $\sqrt{s} = 14$ TeV[♯2] and $p_{\ell\,\mathrm{T}} \ge p_{\ell\,\mathrm{T}}^{min}$, the latter of which leads to the lower bound of E_ℓ as

$$E_\ell \ge p_{\ell\,\mathrm{T}}^{min} / \sqrt{1 - \cos^2\theta_\ell}, \tag{11}$$

[♯2] We performed analyses for $\sqrt{s} = 7$, 8, 10 and 14 TeV in [5], but we here focus on 14 TeV since the LHC is now being upgraded toward this energy.

and Eqs.(10,11) require

$$|\cos\theta_\ell| \leq \sqrt{1 - s(1-\beta)^2 (p_{\ell\,\mathrm{T}}^{min}/m_t^2)^2}. \tag{12}$$

Practically, however, this restriction on $\cos\theta_\ell$ affects its range only a little, e.g., the right-hand side of this inequality is 0.999898 even for $p_{\ell\,\mathrm{T}}^{min} = 100$ GeV.

We show the d_R dependence of the angular distribution within the range $|d_R| \leq 0.1$ [14, 15] in Figs.1–3, where we normalized the distribution by the SM total cross section of the same process but with no $p_{\ell\,\mathrm{T}}$ constraint: $\sigma_{\mathrm{SM}} = 134$ pb, and varied the cut as $p_{\ell\,\mathrm{T}}^{min} = 20$, 30, 40 GeV for $m_t = 173$ GeV. As for d_V we simply set it equal to zero there since what we are interested in is the d_R dependence. Then we show similar curves but for $d_V = -0.01$ [4] (with $d_R = 0$ and no $p_{\ell\,\mathrm{T}}$ cut) in Fig.4 for comparison. In all the Figures, we limit the horizontal range to $|\cos\theta_\ell| \leq 0.5$ simply because the $d_{V,R}$ effects become less clear if we draw the curves over the full range given by Eq.(12).

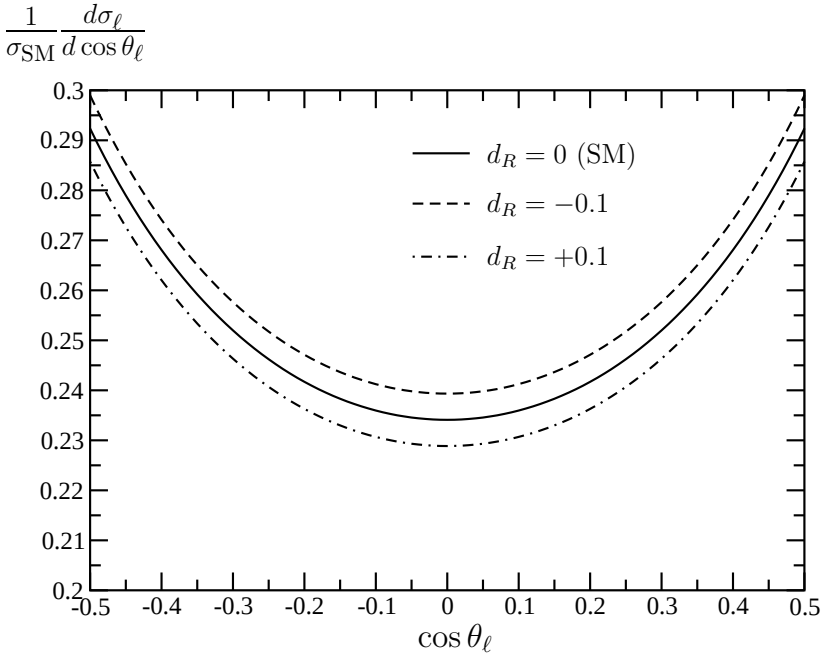

Figure 1: The ℓ^+ angular distributions (without the d_V terms and normalized by the SM total cross section with no $p_{\ell\,\mathrm{T}}$ constraint) for $p_{\ell\,\mathrm{T}}^{min} = 20$ GeV, and $d_R = 0$ (SM), -0.1 and $+0.1$.

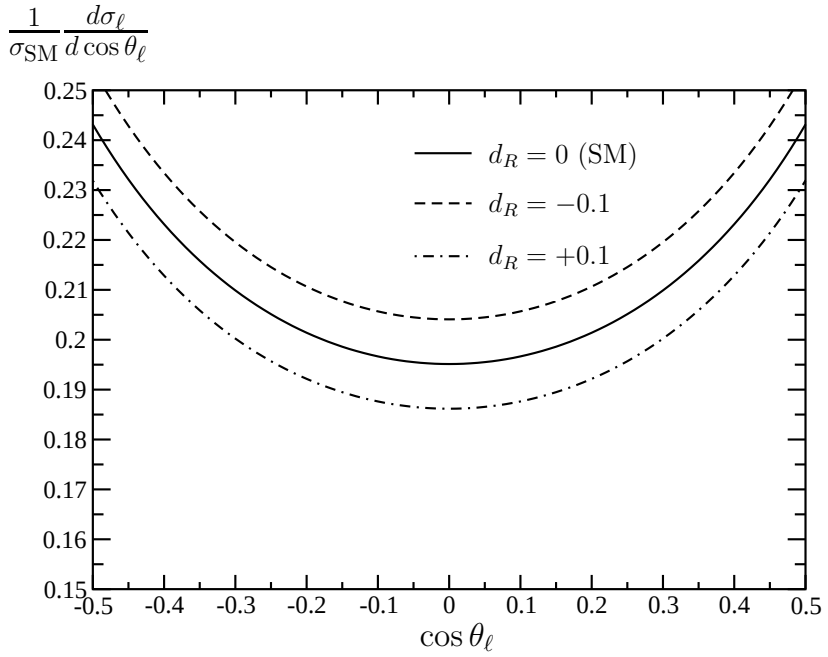

Figure 2: The ℓ^+ angular distributions (without the d_V terms and normalized by the SM total cross section with no $p_{\ell\,\rm T}$ constraint) for $p_{\ell\,\rm T}^{min} = 30$ GeV, and $d_R = 0$ (SM), -0.1 and $+0.1$.

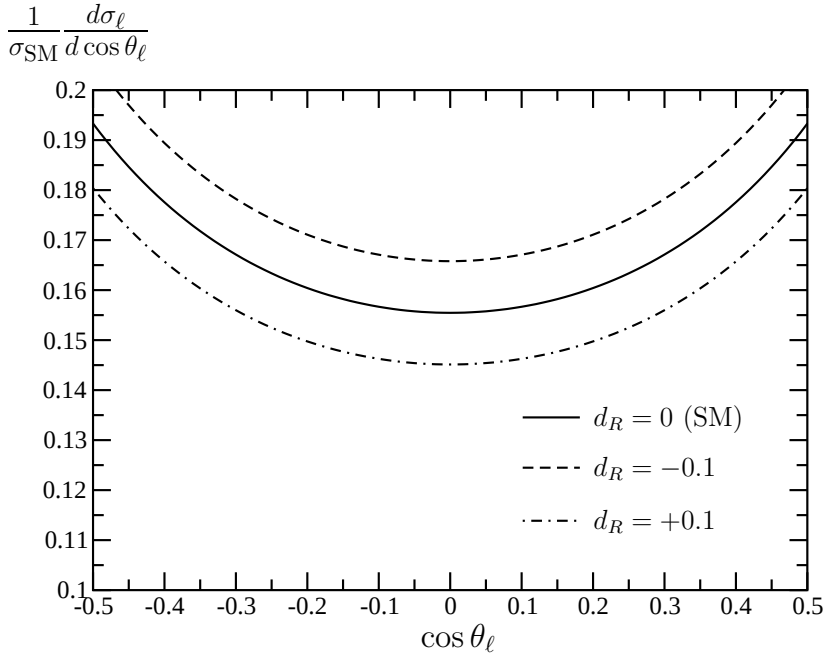

Figure 3: The ℓ^+ angular distributions (without the d_V terms and normalized by the SM total cross section with no $p_{\ell\,\rm T}$ constraint) for $p_{\ell\,\rm T}^{min} = 40$ GeV, and $d_R = 0$ (SM), -0.1 and $+0.1$.

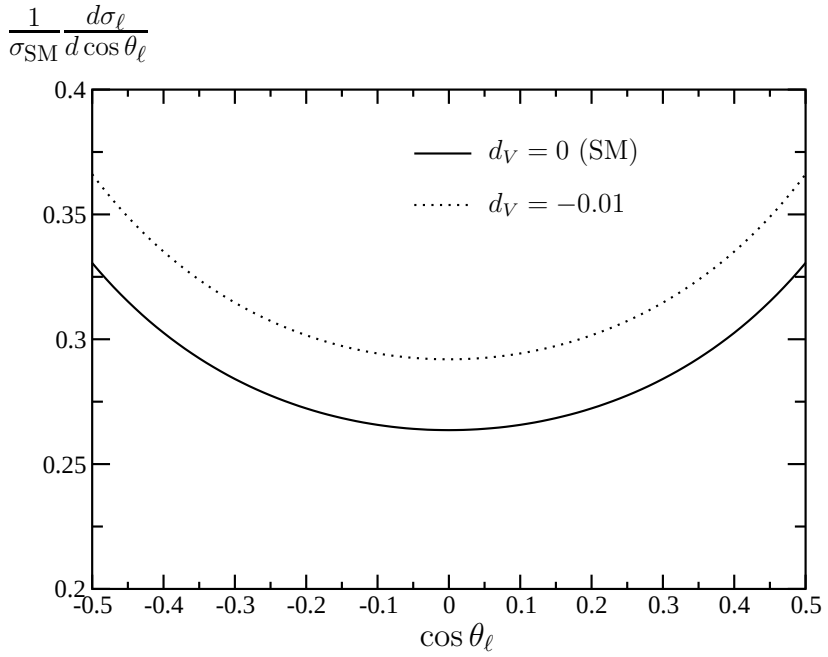

Figure 4: The ℓ^+ angular distributions (without the d_R terms and normalized by the SM total cross section with no $p_{\ell\,\mathrm{T}}$ constraint) for $d_V = 0$ (SM) and -0.01. We did not impose any p_{T} cut here because the d_V effects are free from the decoupling theorem.

We see through Figs.1–3 that the angular distribution with a $p_{\ell\,\mathrm{T}}$ cut has actually become d_R dependent although it is not as large as the d_V contribution in Fig.4. In order to show these $\mathcal{O}(d_R)$ corrections to the SM distributions (with the same $p_{\ell\,\mathrm{T}}$ cut) more quantitatively, let us present their sizes at $\cos\theta_\ell = 0$ for $d_R = 0.1$ as an example:

$$p_{\ell\,\mathrm{T}}^{min} = 20\ \mathrm{GeV}:\ -2.2\,\%, \quad 30\ \mathrm{GeV}:\ -4.6\,\%, \quad 40\ \mathrm{GeV}:\ -6.6\,\%. \tag{13}$$

4. Optimal-observable analysis with $p_{\ell\,\mathrm{T}}$ cut

The optimal-observable analysis (OOA) is a way that could systematically estimate the expected statistical uncertainties of measurable parameters. Here we apply this procedure to the ℓ^+ angular distribution studied in the preceding section.

Leaving its detailed and specific description to [16]–[19], let us show how to compute the uncertainties thereby:

What we have to do first is to calculate the following 3×3 matrix

$$M^c_{ij} \equiv \int d\cos\theta_\ell \frac{g_i(\cos\theta_\ell) g_j(\cos\theta_\ell)}{g_1(\cos\theta_\ell)} \quad (i,\, j = 1,\, 2,\, 3) \tag{14}$$

using $g_{1,2,3}$ defined in Eqs.(8,9), and next its inverse matrix X^c_{ij}, both of which are apparently symmetric.[♯3] This integration is to be performed over the range given by Eq.(12). Then the statistical uncertainties for the measurements of couplings d_V and d_R could be estimated by

$$|\delta d_V| = \sqrt{X^c_{22}\sigma_\ell/N_\ell} = \sqrt{X^c_{22}/L}\,, \tag{15}$$

$$|\delta d_R| = \sqrt{X^c_{33}\sigma_\ell/N_\ell} = \sqrt{X^c_{33}/L}, \tag{16}$$

where σ_ℓ, N_ℓ and L denote the total cross section, the number of events and the integrated luminosity for the process $pp \to t\bar{t}X \to \ell^+ X'$, respectively.

We are now ready to carry out necessary numerical computations. Below we show the elements of M^c computed for $\sqrt{s}$ =14 TeV:

(1) $p^{min}_{\ell\,\mathrm{T}} = 20$ GeV

$$\begin{array}{lll} M^c_{11} = +113.30234, & M^c_{12} = -1207.01858, & M^c_{13} = -28.89719, \\ M^c_{22} = +12861.00330, & M^c_{23} = +306.88261, & M^c_{33} = +7.81915. \end{array} \tag{17}$$

(2) $p^{min}_{\ell\,\mathrm{T}} = 30$ GeV

$$\begin{array}{lll} M^c_{11} = +92.40192, & M^c_{12} = -982.35568, & M^c_{13} = -45.55635, \\ M^c_{22} = +10446.10110, & M^c_{23} = +483.46228, & M^c_{33} = +22.82778. \end{array} \tag{18}$$

(3) $p^{min}_{\ell\,\mathrm{T}} = 40$ GeV

$$\begin{array}{lll} M^c_{11} = +72.29773, & M^c_{12} = -766.31899, & M^c_{13} = -50.54475, \\ M^c_{22} = +8124.55885, & M^c_{23} = +535.07185, & M^c_{33} = +35.59435. \end{array} \tag{19}$$

Here all these results were derived from the cross section in [pb] unit. Using the inverse matrices calculated from these elements, we can estimate the statistical uncertainties of the relevant couplings δd_V and δd_R according to Eqs.(15,16) (Two-parameter analysis).

The set of M^c_{ij} (17)–(19) also enables us to give another numerical results. That is, we can do a similar analysis but assuming only d_R is unknown. This

[♯3] In our preceding OOA [5], we distinguished those quantities computed from the angular and energy distributions by adding them superscripts "c" and "E" respectively. Here we do not need such a superscript but we left it for easy comparison with our previous results.

assumption is never unreasonable because we already have shown that we would be able to obtain good information on d_V (and d_A) through the total cross section of $pp/p\bar{p} \to t\bar{t}X$ without being affected by the top-decay processes. All we have to do for that is perform the same computations but without the d_V component, i.e., compute the 2×2 matrix X^c_{ij} from M^c_{ij} with $i, j = 1, 3$, and use Eq.(16) (One-parameter analysis).

Before giving the results, however, we should remember that we encountered an instability problem when computing the inverse-matrix in our previous analysis [5]. That is, the numerical results fluctuated to a certain extent (beyond our expectation) depending on to which decimal places of $M^{c,E}$ we take into account as our input data. Therefore we compute here X^c_{ii} not only for the above M^c_{ij} but also for those to three and one decimal places in order to check to what extent the results are stable:

• Two-parameter analysis

(1) $p_{\ell\,\mathrm{T}}^{min} = 20$ GeV

$$X^c_{22} = 2.1\,(2.3,\ 2.2), \quad X^c_{33} = 11.7\,(12.6,\ 14.0). \tag{20}$$

(2) $p_{\ell\,\mathrm{T}}^{min} = 30$ GeV

$$X^c_{22} = 3.1\,(2.9,\ ***), \quad X^c_{33} = 19.7\,(18.4,\ ***). \tag{21}$$

(3) $p_{\ell\,\mathrm{T}}^{min} = 40$ GeV

$$X^c_{22} = 5.2\,(4.7,\ 0.4), \quad X^c_{33} = 40.0\,(36.2,\ 3.1). \tag{22}$$

Here all the figures in the parentheses are from M^c_{ij} rounded off properly to three and one decimal places respectively, and $***$ expresses that we had no meaningful solutions there, i.e., the results became negative. The results for $p_{\ell\,\mathrm{T}}^{min} = 20$ GeV seem to be rather stable, but there is non-negligible instability in the results for $p_{\ell\,\mathrm{T}}^{min} = 30$ and 40 GeV. Therefore we conclude that we would not obtain reliable results from the two-parameter analysis unless the corresponding cross sections are determined very precisely, i.e., at least to three-decimal-place precision. As discussed in [5], this problem would come from dominant d_V-term contributions.

Indeed, the following results of the one-parameter analysis without the d_V term are quite stable.

• One-parameter analysis

(1) $p_{\ell\,\mathrm{T}}^{min} = 20$ GeV

$$X_{33}^{c} = 2.2\,(2.2,\ 2.3). \tag{23}$$

(2) $p_{\ell\,\mathrm{T}}^{min} = 30$ GeV

$$X_{33}^{c} = 2.7\,(2.7,\ 3.4). \tag{24}$$

(3) $p_{\ell\,\mathrm{T}}^{min} = 40$ GeV

$$X_{33}^{c} = 3.9\,(3.9,\ 3.1). \tag{25}$$

These results present us a hint for anomalous-top-couplings search through the lepton angular distribution, i.e., it will be effective (and also inevitable) to combine its data with those of the total $t\bar{t}$ cross section where we will be able to explore d_V (and also d_A) in detail.

Let us present our final results for the one-parameter analysis. The expected statistical uncertainties in measuring d_R are estimated as follows:

(1) $p_{\ell\,\mathrm{T}}^{min} = 20$ GeV

$$|\delta d_R| = (1.5 \pm 0.0)/\sqrt{L}. \tag{26}$$

(2) $p_{\ell\,\mathrm{T}}^{min} = 30$ GeV

$$|\delta d_R| = (1.7 \pm 0.1)/\sqrt{L}. \tag{27}$$

(3) $p_{\ell\,\mathrm{T}}^{min} = 40$ GeV

$$|\delta d_R| = (1.9 \pm 0.1)/\sqrt{L}. \tag{28}$$

For instance, if $L = 1000$ pb^{-1} is achieved and if there exists nonstandard d_R coupling with the size $d_R = 0.1$, we would be able to confirm its effects at 2.1σ level (apart from the systematic errors) via an analysis using $p_{\ell\,\mathrm{T}}^{min} = 20$ GeV.

Finally, before closing this section, another comment would be also necessary on QCD higher-order corrections since all the numerical computations here were done with the tree-level formulas. In order to take into account those corrections, we multiply the tree cross sections by the K-factor ($K \simeq 1.5$ [20]). This factor disappears in the combination $X_{ii}^{c}\sigma_\ell$ and remains only in $N_\ell\,(= L\sigma_\ell)$ when we estimate $\delta d_{V,R}$. Therefore the luminosity L in our results should be understood as

an effective one including K (and also the final charged-lepton detection-efficiency ϵ_ℓ).

5. Summary

We studied possible nonstandard top-gluon and top-W couplings for hadron-collider experiments through the angular distribution of the final charged-lepton from a top-quark semileptonic decay in a model-independent way. Those couplings are derived as parameters which characterize the effects of dimension-6 effective operators based on the scenario of Buchmüller and Wyler [9]. More specifically, we analyzed the top-gluon coupling (denoted as d_V) and the top-W coupling (denoted as d_R) which contribute to top-quark pair productions and decays respectively in the linear approximation as nonstandard interactions.

We are not able to observe the d_R-term contribution through the lepton angular distribution due to the decoupling theorem [6]–[8], if we perform the lepton-energy integration fully over the kinematically-allowed range when deriving this distribution. Our main purpose here was to explore if we could draw any new information on d_R via an optimal-observable analysis of this distribution by introducing a lepton transverse-momentum cut and giving the angular distribution some d_R dependence.

We found that the distribution thereby becomes actually d_R dependent, which enabled us to carry out an optimal-observable analysis including the d_R-terms, although we encountered an instability problem in calculating necessary inverse-matrices as in our preceding study [5]. Therefore we will be able to obtain some new information on this parameter. In fact, this $p_{\ell\,\mathrm{T}}$ constraint makes the corresponding cross section smaller and consequently the precision becomes a bit lower than the case of the analysis using the lepton energy distribution [5]. However we still would like to stress that the analyses here are useful since we should combine all available data in order to explore possible new physics beyond the standard model.

Acknowledgments

This work was partly supported by the Grant-in-Aid for Scientific Research No. 22540284 from the Japan Society for the Promotion of Science. Part of the algebraic and numerical calculations were carried out on the computer system at Yukawa

Institute for Theoretical Physics (YITP), Kyoto University.

REFERENCES

[1] LHC website: `http://public.web.cern.ch/public/en/LHC/LHC-en.html`

[2] Z. Hioki and K. Ohkuma, Eur. Phys. J. C **65** (2010) 127 (arXiv:0910.3049 [hep-ph]); *ibid.* C **71** (2011) 1535 (arXiv:1011.2655 [hep-ph]).

[3] Z. Hioki and K. Ohkuma, Phys. Rev. D **83** (2011) 114045 (arXiv:1104.1221 [hep-ph]);

[4] Z. Hioki and K. Ohkuma, Phys. Rev. D **88** (2013) 017503 (arXiv:1306.5387 [hep-ph]).

[5] Z. Hioki and K. Ohkuma, Phys. Lett. B **716** (2012) 310 (arXiv:1206.2413 [hep-ph]).

[6] B. Grzadkowski and Z. Hioki, Phys. Lett. B **476** (2000) 87 (hep-ph/9911505); *ibid.* B **529** (2002) 82 (hep-ph/0112361); *ibid.* B **557** (2003) 55 (hep-ph/0208079).

[7] S.D. Rindani, Pramana **54** (2000) 791 (hep-ph/0002006).

[8] R.M. Godbole, S.D. Rindani and R.K. Singh, JHEP **0612** (2006) 021 (hep-ph/0605100).

[9] W. Buchmuller and D. Wyler, Nucl. Phys. B **268** (1986) 621.

[10] C. Arzt, M.B. Einhorn and J. Wudka, Nucl. Phys. B **433** (1995) 41 (hep-ph/9405214).

[11] J.A. Aguilar-Saavedra, Nucl. Phys. B **812** (2009) 181 (arXiv:0811.3842 [hep-ph]); *ibid.* B **821** (2009) 215 (arXiv:0904.2387 [hep-ph]).

[12] B. Grzadkowski, M. Iskrzynski, M. Misiak and J. Rosiek, JHEP **1010** (2010) 085 (arXiv:1008.4884 [hep-ph]).

[13] P.M. Nadolsky, H.-L. Lai, Q.-H. Cao, J. Huston, J. Pumplin, D. Stump, W.-K. Tung and C.-P. Yuan, Phys. Rev. D **78** (2008) 013004 (arXiv:0802.0007 [hep-ph]).

[14] B. Grzadkowski and M. Misiak, Phys. Rev. D **78** (2008) 077501 [Erratum-ibid. D **84** (2011) 059903] (arXiv:0802.1413 [hep-ph]).

[15] A. Prasath, R.M. Godbole and S.D. Rindani, arXiv:1405.1264 [hep-ph].

[16] D. Atwood and A. Soni, Phys. Rev. D **45** (1992) 2405.

[17] M. Davier, L. Duflot, F. Le Diberder and A. Rouge, Phys. Lett. B **306** (1993) 411.

[18] M. Diehl and O. Nachtmann, Z. Phys. C **62** (1994) 397.

[19] J.F. Gunion, B. Grzadkowski and X.-G. He, Phys. Rev. Lett. **77** (1996) 5172 (hep-ph/9605326).

[20] N. Kidonakis, arXiv:1311.0283 [hep-ph].